JACS
JOURNAL OF THE AMERICAN CHEMICAL SOCIETY

Communication

pubs.acs.org/JACS

DNA-Based Self-Assembly of Fluorescent Nanodiamonds

Tao Zhang,[†] Andre Neumann,[†] Jessica Lindlau,[†] Yuzhou Wu,[‡] Goutam Pramanik,[‡] Boris Naydenov,[§] Fedor Jelezko,[§] Florian Schüder,[†] Sebastian Huber,[†] Marinus Huber,[†] Florian Stehr,[†] Alexander Högele,*[,†] Tanja Weil,*[,‡] and Tim Liedl*[,†]

[†]Faculty of Physics and Center for NanoScience (CeNS), Ludwig-Maximilians-Universität München, Geschwister-Scholl-Platz 1, D-80539 München, Germany

[‡]Institute for Organic Chemistry III/Macromolecular Chemistry and [§]Institute for Quantum Optics, Universität Ulm, Albert-Einstein-Allee 11, D-89081 Ulm, Germany

Supporting Information

ABSTRACT: As a step toward deterministic and scalable assembly of ordered spin arrays we here demonstrate a bottom-up approach to position fluorescent nanodiamonds (NDs) with nanometer precision on DNA origami structures. We have realized a reliable and broadly applicable surface modification strategy that results in DNA-functionalized and perfectly dispersed NDs that were then self-assembled in predefined geometries. With optical studies we show that the fluorescence properties of the nitrogen-vacancy color centers in NDs are preserved during surface modification and DNA assembly. As this method allows the nanoscale arrangement of fluorescent NDs together with other optically active components in complex geometries, applications based on self-assembled spin lattices or plasmon-enhanced spin sensors as well as improved fluorescent labeling for bioimaging could be envisioned.

Fluorescent nanodiamonds (FNDs) constitute a new class of stable fluorescent markers, which show neither photobleaching nor blinking and are at the same time biocompatible due to a chemically robust and inert surface.[1] This renders FNDs perfectly suited for a wide range of biocompatible applications[2] including thermometry,[3] imaging and tracking,[4] or super-resolution microscopy.[5] On the other hand, remarkably long electron spin coherence times of nitrogen-vacancy (NV) color centers in diamond[6] provide a promising platform for nanoscale spin-based quantum technologies such as magnetometry[7] and information processing.[8] Importantly, the spin state associated with single NV centers can be initiated, manipulated, and read-out optically even at room temperature, which renders such color centers ideal candidates for studying spin−spin interactions.[9]

Nanodiamonds (NDs) can be obtained through detonation reaction, milling of large diamond crystals or chemical vapor deposition.[10] The optically active defects in NDs—also called color centers—are created by doping impurities into the atomic diamond lattice, a process that usually involves ion implantation and annealing treatment at high temperature. Up to 500 different color centers associated with specific impurities have been identified, and many have been extensively studied with optical spectroscopy techniques.[11] One particular type of defect, the NV center, has emerged as a platform for quantum information processing and biosensing applications.[1] NV centers are prepared by replacing two adjacent carbon positions in the atomic lattice of sp^3 allotrope of carbon: one with nitrogen and the other with a vacancy. Upon fluorescence excitation these color centers emit a characteristic zero-phonon line at 637 nm accompanied by Stokes and anti-Stokes phonon sidebands.

The continuing development of the above-stated applications of NV centers strongly relies on the controlled conjugation of the color centers to defined target sites or their controlled arrangement in space. To date, spatial organization of FNDs was realized in a using an atomic force microscope and on protein arrays.[12] As a powerful alternative, DNA-based nanostructuring[13] provides a bottom-up method to precisely position NDs in space. Based on selective Watson−Crick base pairings, arbitrary 2D or 3D DNA nanostructures[14] can be designed[15] and manufactured, which can further direct the assembly of nanoscale materials such as carbon nanotubes,[16] metal nanoparticles,[17] quantum dots,[18] and proteins.[19] Such composite assemblies based on DNA nanostructures offer an ideal platform to study the distance- and orientation-dependent electronic and optical properties of nanoparticles[18b] or the enzymatic activity of biomolecular assemblies.[19b] Until now, low colloidal stability at high ionic strengths even of coated FNDs has prohibited their conjugation to DNA nanostructures.

Previously reported acidic treatment for NDs removes disordered carbon and creates reactive species such as ketone, hydroxyl, carboxyl, etc.[3,20] However, only a limited number of carboxyl groups can be obtained which limits direct surface conjugation with amine-modified single-stranded DNA and hence did not yield stable complexes in our experiments (data not shown).

Inspired by layer-by-layer assembly where multicomposite surfaces are built using the electrostatic attraction between oppositely charged molecules,[21] we have then modified the NDs by exploiting multiple charge interactions. Briefly, an amphiphilic biopolymer[22] derived from denatured bovine serum albumin (dBSA) with grafted polyethylene glycol (PEG) chains terminated with biotin or methoxy groups was employed offering both stabilizing electrostatic and hydro-

Received: May 18, 2015
Published: July 21, 2015

DOI: 10.1021/jacs.5b04857
J. Am. Chem. Soc. 2015, 137, 9776−9779

phobic interactions. After overnight stirring in 0.5 × TBE buffer with NDs and dBSA-PEG and then purification by centrifugation, dBSA-PEG-modified NDs were obtained (SI Methods, Notes S1 and S2, Tables S1 and S2). With our approach we have realized for the first time a biopolymer-based coating that efficiently encapsulates NDs and imparts high colloidal stability even at high ionic strength required for DNA conjugation. Most importantly, multiple functional groups can be introduced to the FNDs' surface providing now access to site-specific bioconjugation to precisely assemble FNDs with DNA origami.

Due to the steric repulsion effect of the grafted PEG chains, the dBSA-PEG-coated NDs were fully dispersed in TBE buffer even in the presence of 10 mM $MgCl_2$ (Figure 1 and Figure S1). Note that TEM images revealed strong clustering of the untreated NDs after drying on the carbon-coated Formvar grids, and no reliable image analysis was possible. After treatment with dBSA-PEG, however, the NDs were perfectly dispersed, and we measured an average diameter of the NDs of 49.0 ± 14 nm. NDs grafted with PEG3000 revealed a surface-to-surface distance of 149 ± 37 nm, while NDs modified with the shorter PEG750 molecules exhibited a shorter separation distance of 48.0 ± 12 nm (Figure 1c,d, Figures S2 and S3). Importantly, the distance distribution was sharp enough to allow for the formation of lattice-like assemblies as can be seen in Figure 1c,d.

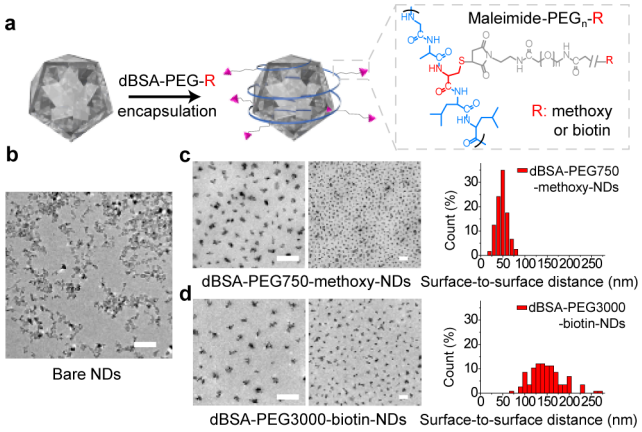

Figure 1. Surface modification of NDs. (a) dBSA-PEG-R (R: methoxy or biotin) is conjugated to the NDs via charge and hydrophobic interactions.(b) TEM images of bare NDs. Note that mainly clusters are observed before coating. (c) TEM images of NDs modified with dBSA-PEG750-methoxy. This coating results in perfect dispersion of the NDs and an average surface-to-surface distance of 48 ± 12 nm.(d) TEM images of NDs modified with dBSA-PEG3000-biotin. The longer PEG-chains increase the observed average surface-to-surface distance to 149 nm (scale bars: 200 nm).

Dynamic light scattering (DLS) measurements were carried out to observe the size changes of the NDs after surface modification in solution (Figure S4). Note that DLS of bare NDs could only be performed after spinning down aggregates. The averaged hydrodynamic diameters of the NDs increased from 97 to 120 nm, while the size distribution decreased from 124 to 107 nm (full width at half maximum, fwhm) before and after coating with dBSA-PEG3000-biotin, respectively. These observations indicate that clusters were still present during the DLS measurement of bare NDs and that the coating procedure homogenized the size distribution. The surface potential increased from −28.2 ± 14.2 mV for untreated NDs to −7.6 ± 7.03 mV after polymer coating, which indicates that the surface functionalization is also based on charge interactions with the positively charged BSA backbone partially neutralizing the negatively charged ND surface. Fourier transform infrared spectroscopy (FTIR) and X-ray photoelectron spectroscopy (XPS) of dBSA-PEG-modified NDs exhibit significant signals of PEG and dBSA molecules and two different types of sulfur atoms, respectively, indicating the successful coating (Figures S5 and S6).

To spatially organize our coated FNDs we chose four different DNA origami structures: a six-helix bundle[23] (6HB, 428 nm long), a 14-helix bundle[18b] (14HB, 210 nm long), a 24-helix bundle[17b] (24HB, 100 nm long), and a 2-layered sheet (2LS, 50 nm × 50 nm). Biotin-labeled oligonucleotides extending from the DNA structures either at their ends or their sides served as anchor sites for neutravidin molecules, each of which offered four binding sites to biotin (Figure 2a,b and Methods in SI). The remaining unoccupied biotin pockets were then used to conjugate biotin residues of the biotin-functionalized FNDs (dBSA-PEG3000-biotin modified FNDs). Due to the multivalent nature of the biotin-FNDs, varying morphologies were observed dependent on the ratio of the mixed components (Figures S7−S9). By fine-tuning the ratio of biotin-FNDs and DNA origami structures for each batch of FNDs, the assembly yield of FND dimers was optimized. TEM analysis revealed a yield of correctly assembled dimers of up to 27% (Table S3) and confirmed the efficient control over the separation distances of FNDs dimers: 96 ± 24 nm (SD) for 24HBs, 208 ± 28 nm for 14HBs, and 361 ± 40 nm for 6HBs (Figure 2c−e). The 6HBs consist of only six parallel DNA helices and are therefore more flexible than the 14HBs or 24HBs (14 and 24 parallel helices).[24] As a result of their flexibility, many of the 6HBs adsorb on the TEM grid in bent configurations that have shorter end-to-end distances than a fully stretched bundle, and thus large deviations from the nominal length are observed. The flexible PEG-linkages that connect the FNDs to the DNA constructs additionally contribute to a random distribution of distances for all bundle types.

As DNA origami allows the formation of virtually any geometry, the spatial organization of FNDs is not limited to dimer assemblies. Figure 2f,g shows FNDs that were designed to arrange in a triangle and an irregular tetrahedron, respectively. For these geometries, we offered either three or four binding sites at the edges of the two-layered sheet as depicted in the schematic drawings. TEM revealed the successful assembly of clusters of three and four NDs. Note that due to the flattening of the structures during adsorption to the TEM grid, we were not able to prove the three dimensionality of the tetrahedron design.

Finally, we explored the optical properties of the self-assembled FND dimers containing NV centers in a confocal microfluorescence spectroscopy setup under ambient conditions (SI Methods, Note S3). A representative color-coded fluorescence intensity map of spatially dispersed FND dimer nanostructures (6HBs) on quartz is shown in Figure 3a. The map was recorded with diffraction-limited confocal excitation at 532 nm and collection above 575 nm by raster scanning the sample with respect to the focal spot (fwhm spot size of ∼370 nm). Several FND dimer assemblies appear as pairs of fluorescence hotspots in the map. Other assemblies are not clearly resolvable or represent single-labeled 6HBs. Figure 3b,c

DOI: 10.1021/jacs.5b04857
J. Am. Chem. Soc. 2015, 137, 9776−9779

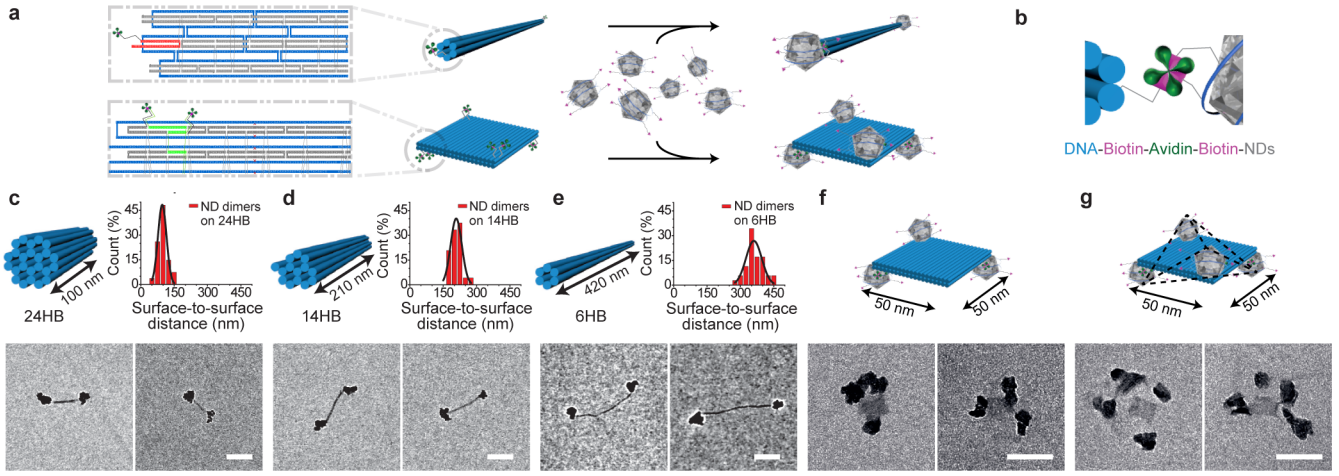

Figure 2. Self-assembly of NDs with DNA origami. (a) DNA sequence maps (SI Note S4) exemplarily show design details of binding sites on the six-helix bundle and the two-layered sheet. By mixing the biotin-functionalized NDs with the neutravidin-modified DNA structures, the biotin residues of the modified NDs bind to the remaining free pockets of the neutravidin, which leads to the site-specific assembly of NDs.(b) Schematic conjugation between NDs and DNA origami. (c–g) Top: DNA nanostructure design and histograms (with Gaussian fits) of the NDs surface-to-surface distance. (c) 24-helix bundles yield an average distance of 96 nm (designed distance: 100 nm).(d) 14-helix bundles yield an average distance of 208 nm (designed distance: 210 nm). (e) 6-helix bundle yield an average distance of 361 nm (designed distance: 428 nm. Note that this DNA construct is considerably more flexible compared to the other two). (f, g) NDs trimer and tetramer assembly on a two-layered origami sheet (50 × 50 nm). Bottom: corresponding TEM images of ND assemblies (Scale bars: 100 nm).

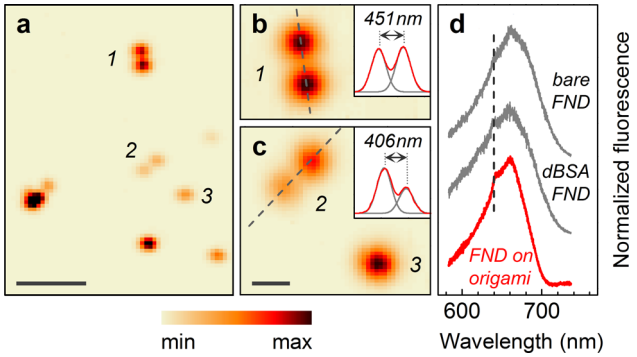

Figure 3. Optical analysis of DNA origami-assembled fluorescent NDs. (a) Color-coded confocal fluorescence map of ND dimers (6HB). The dimer assemblies appear as pairs or individual fluorescence hotspots in the confocal map. Scale bar: 2 μm. (b, c) Zoom-in on ND dimers with corresponding line scans fitted with two gaussians. Scale bar: 400 nm. (d) Fluorescence spectrum of a ND assembled on DNA origami (red trace) together with typical spectra of a bare and a dBSA-PEG3000-biotin-modified ND (gray traces). The spectra are offset for clarity to highlight the characteristics of negatively charged NV center fluorescence, which was unaffected by our procedures. Note that the reduced intensity of the long-wavelength phonon side-bands is a result of the chromatic optical response function of the setup.

depicts two high-resolution maps of FND dimers exhibiting a separation of 451 and 406 nm, which is well within the limits of an expected maximum center-to-center distance of ~476 nm (length of 6HB + radius of coated FND: 428 + 48 nm). Figure 3d shows a typical spectrum of an FND assembled on DNA origami (red trace) (see Figure S10 for further spectra). It exhibits spectral characteristics of negatively charged NV color centers in diamond with a noticeable zero-phonon line at 637 nm (NV^-) accompanied by Stokes and anti-Stokes phonon-sidebands. For comparison, we also present typical spectra of a bare (upper gray trace) and a dBSA-PEG3000-biotin-modified (lower gray trace) FND. All spectra exhibit the same features indicating that the fluorescence properties of FNDs are robust against the dBSA-PEG modification and the DNA assembly procedures (see Figure S11 for complementary examples and Figure S12 for a spectral time trace).

In conclusion, we have successfully realized nanoscale positioning of NDs containing fluorescent NV-centers by DNA self-assembly. Bioconjugation betweeen FNDs and DNA could be accomplished by a PEG-labeled biopolymer surface coating derived from the plasma protein BSA that imparts high colloidal stability to the FND. This approach offers the possibility to introduce many different modifications at the same time by attaching the desired end groups to the PEG molecules, as demonstrated herein for biotin. Fluorescence measurements certified correct assembly and that our method does not alter the optical properties of the NV centers. Moreover, using DNA origami, FNDs could be arranged in nanoscale geometries with other optically active nanoparticles. Since NV centers exhibit excellent photostability and remarkably long electron spin coherence times for efficient spin manipulation by optical means, site-specific arrangement of FNDs would ultimately allow investigating the coherent coupling of NV centers assembled in pairs and extended arrays or lattices, which is a step toward the realization of scalable quantum processors and simulators.[12b] Before this goal can be approached with the method presented here, however, thinner coating layers for the FNDs have to be developed, and the positioning accuracy as well as efficiency has to be increased further.

■ ASSOCIATED CONTENT

Supporting Information

The Supporting Information is available free of charge on the ACS Publications website at DOI: 10.1021/jacs.5b04857.

Methods and materials, additional data including DLS measurements, TEM images, optical analysis, and DNA origami design (PDF)

DOI: 10.1021/jacs.5b04857
J. Am. Chem. Soc. 2015, 137, 9776–9779

AUTHOR INFORMATION

Corresponding Authors

*alexander.hoegele@physik.uni-muenchen.de
*tanja.weil@uni-ulm.de
*tim.liedl@physik.lmu.de

Notes

The authors declare no competing financial interest.

ACKNOWLEDGMENTS

Financial support by the Volkswagen Foundation, the DAAD, the DFG Excellence Initiative via the Nanosystems Initiative Munich (NIM), and the Center for NanoScience (CeNS) is gratefully acknowledged. T.W. and F.J. are grateful to the financial support from the ERC Synergy Grant 319130-BioQ. We thank Martin Plenio for discussions on self-organized ND arrays, Miao Li for DLS measurements, Susanne Kemper for TEM instructions, and Milena Mayer for figure preparation.

REFERENCES

(1) Aharonovich, I.; Greentree, A. D.; Prawer, S. *Nat. Photonics* **2011**, *5*, 397.
(2) Schrand, A. M.; Hens, S. A. C.; Shenderova, O. A. *Crit. Rev. Solid State Mater. Sci.* **2009**, *34*, 18.
(3) Kucsko, G.; Maurer, P. C.; Yao, N. Y.; Kubo, M.; Noh, H. J.; Lo, P. K.; Park, H.; Lukin, M. D. *Nature* **2013**, *500*, 54.
(4) Ritterger, E.; Han, K. Y.; Irvine, S. E.; Eggeling, C.; Hell, S. W. *Nat. Photonics* **2009**, *3*, 144.
(5) Chang, Y.−R.; Lee, H.−Y.; Chen, K.; Chang, C.−C.; Tsai, D.−S.; Fu, C.−C.; Lim, T.−S.; Tzeng, Y.−K.; Fang, C.−Y.; Han, C.−C.; Chang, H.−C.; Fann, W. *Nat. Nanotechnol.* **2008**, *3*, 284.
(6) Balasubramanian, G.; Neumann, P.; Twitchen, D.; Markham, M.; Kolesov, R.; Mizuochi, N.; Isoya, J.; Achard, J.; Beck, J.; Tissler, J.; Jacques, V.; Hemmer, P. R.; Jelezko, F.; Wrachtrup, J. *Nat. Mater.* **2009**, *8*, 383.
(7) (a) Maze, J. R.; Stanwix, P. L.; Hodges, J. S.; Hong, S.; Taylor, J. M.; Cappellaro, P.; Jiang, L.; Dutt, M. V.; Togan, E.; Zibrov, A. S.; Yacoby, A.; Walsworth, R. L.; Lukin, M. D. *Nature* **2008**, *455*, 644. (b) Balasubramanian, G.; Chan, I. Y.; Kolesov, R.; Al−Hmoud, M.; Tisler, J.; Shin, C.; Kim, C.; Wojcik, A.; Hemmer, P. R.; Krueger, A.; Hanke, T.; Leitenstorfer, A.; Bratschitsch, R.; Jelezko, F.; Wrachtrup, J. *Nature* **2008**, *455*, 648.
(8) Fuchs, G. D.; Burkard, G.; Klimov, P. V.; Awschalom, D. D. *Nat. Phys.* **2011**, *7*, 789.
(9) Gaebel, T.; Domhan, M.; Popa, I.; Wittmann, C.; Neumann, P.; Jelezko, F.; Rabeau, J. R.; Stavrias, N.; Greentree, A. D.; Prawer, S.; Meijer, J.; Twamley, J.; Hemmer, P. R.; Wrachtrup, J. *Nat. Phys.* **2006**, *2*, 408.
(10) Mochalin, V. N.; Shenderova, O.; Ho, D.; Gogotsi, Y. *Nat. Nanotechnol.* **2011**, *7*, 11.
(11) Zaitsev, A. M. *Phys. Rev. B: Condens. Matter Mater. Phys.* **2000**, *61*, 12909.
(12) (a) Schietinger, S.; Barth, M.; Aichele, T.; Benson, O. *Nano Lett.* **2009**, *9*, 1694. (b) Albrecht, A.; Koplovitz, G.; Retzker, A.; Jelezko, F.; Yochelis, S.; Porath, D.; Nevo, Y.; Shoseyov, O.; Paltiel, Y.; Plenio, M. B. *New J. Phys.* **2014**, *16*, 09302.
(13) (a) Seeman, N. C. *J. Theor. Biol.* **1982**, *99*, 237. (b) Seeman, N. C. *Annu. Rev. Biochem.* **2010**, *79*, 65.
(14) (a) Rothemund, P. W. K. *Nature* **2006**, *440*, 297. (b) Douglas, S. M.; Dietz, H.; Liedl, T.; Hogberg, B.; Graf, F.; Shih, W. M. *Nature* **2009**, *459*, 414.
(15) Douglas, S. M.; Marblestone, A. H.; Teerapittayanon, S.; Vazquez, A.; Church, G. M.; Shih, W. M. *Nucleic Acids Res.* **2009**, *37*, 5001.
(16) Maune, H. T.; Han, S.−p.; Barish, R. D.; Bockrath, M.; Goddard, I. I. A.; Rothemund, P. W. K.; Winfree, E. *Nat. Nanotechnol.* **2010**, *5*, 61.
(17) (a) Zheng, J.; Constantinou, P. E.; Micheel, C.; Alivisatos, A. P.; Kiehl, R. A.; Seeman, N. C. *Nano Lett.* **2006**, *6*, 1502. (b) Kuzyk, A.; Schreiber, R.; Fan, Z.; Pardatscher, G.; Roller, E.−M.; Hogele, A.; Simmel, F. C.; Govorov, A. O.; Liedl, T. *Nature* **2012**, *483*, 311.
(18) (a) Deng, Z.; Samanta, A.; Nangreave, J.; Yan, H.; Liu, Y. *J. Am. Chem. Soc.* **2012**, *134*, 17424. (b) Schreiber, R.; Do, J.; Roller, E.-M.; Zhang, T.; Schüller, V. J.; Nickels, P. C.; Feldmann, J.; Liedl, T. *Nat. Nanotechnol.* **2013**, *9*, 74.
(19) (a) Voigt, N. V.; Torring, T.; Rotaru, A.; Jacobsen, M. F.; Ravnsbaek, J. B.; Subramani, R.; Mamdouh, W.; Kjems, J.; Mokhir, A.; Besenbacher, F.; Gothelf, K. V. *Nat. Nanotechnol.* **2010**, *5*, 200. (b) Fu, J.; Yang, Y. R.; Johnson-Buck, A.; Liu, M.; Liu, Y.; Walter, N. G.; Woodbury, N. W.; Yan, H. *Nat. Nanotechnol.* **2014**, *9*, 531. (c) Udomprasert, A.; Bongiovanni, M. N.; Sha, R.; Sherman, W. B.; Wang, T.; Arora, P. S.; Canary, J. W.; Gras, S. L.; Seeman, N. C. *Nat. Nanotechnol.* **2014**, *9*, 537.
(20) Krueger, A.; Lang, D. *Adv. Funct. Mater.* **2012**, *22*, 890.
(21) Decher, G. *Science* **1997**, *277*, 1232.
(22) Wu, Y.; Chakrabortty, S.; Gropeanu, R. A.; Wilhelmi, J.; Xu, Y.; Er, K. S.; Kuan, S. L.; Koynov, K.; Chan, Y.; Weil, T. *J. Am. Chem. Soc.* **2010**, *132*, 5012.
(23) Douglas, S. M.; Chou, J. J.; Shih, W. M. *Proc. Natl. Acad. Sci. U. S. A.* **2007**, *104*, 6644.
(24) (a) Liedl, T.; Högberg, B.; Tytell, J.; Ingber, D. E.; Shih, W. M. *Nat. Nanotechnol.* **2010**, *5*, 520. (b) Kauert, D. J.; Kurth, T.; Liedl, T.; Seidel, R. *Nano Lett.* **2011**, *11*, 5558.

DOI: 10.1021/jacs.5b04857
J. Am. Chem. Soc. 2015, 137, 9776−9779